Available online at www.sciencedirect.com

ScienceDirect

Procedia Engineering 105 (2015) 192 – 200

Procedia Engineering

www.elsevier.com/locate/procedia

6th BSME International Conference on Thermal Engineering (ICTE 2014)

Analysis of Heat Transfer in Channel Flow Subject to Sine-Bump Heating

Umera Sarjana[a], M. Zakir Hossain[b], AKM Monjur Morshed[a]

[a]Department of Mechanical Engineering, Bangladesh University of Engineering and Technology (BUET), Dhaka.
[b]Department of Mechanical and Materials Engineering, University of Western Ontario, Ontario, Canada.
umera.sarjana@gmail.com[a] zakir92@yahoo.com[b] mmmsumon@gmail.com[a]

Abstract

Convection in a channel subject to a distributed sinusoidal bump like heating applied at the lower wall has been studied. It is found that small wave number heating provides large plumes whereas large wave number heating provides a uniform temperature distribution at the upper part of the channel. Heat transfer is more efficient at low Reynolds number with small wave number heating.

Peer-review under responsibility of organizing committee of the 6th BSME International Conference on Thermal Engineering (ICTE 2014)

Keywords: Convection; Heating; Reynolds number; sinusoidal bump;

1.Introduction

A fluid layer bounded by two parallel plates heated uniformly from below represents a classical system known as Rayleigh-Benard (RB) convection [1]. It is known that this convection motion starts when the temperature difference between the plates reaches a critical value. Below this critical point the heat is transported between the plates by conduction and the temperature changes linearly across the layer. Above this critical point the heat transfer rate is increased by the thermal instability and the temperature field is strongly influenced by the presence of convective roll vortices.

* AKM Monjur Morshed. Tel.:+8801795075520;
*E-mail address:*monjur_morshed@me.buet.ac.com

Peer-review under responsibility of organizing committee of the 6th BSME International Conference on Thermal Engineering (ICTE 2014)
doi:10.1016/j.proeng.2015.05.055

These roll vortices assists to augment the heat transfer process in the case of forced convection [2]. In some applications, the bump-like heating is combined with a forced motion resulting in a mixed convection. Such convection is most likely to occur in many system of practical importance.Some of the examples of spatially distributed heating are included in the presence of ocean and land in the earth, presence of local lakes, a set of local fires, a set of computer chips, a set of electrically heated wires inserted on a surface etc [3]. Such systems are modeled using an infinite slot subjected to periodic variation of the temperature defined by sinusoidal-bump-like function at the bottom wall.

Convection driven by a periodic heating, defined by a simple sinusoidal function, in the absence of mean temperature gradient has been studied by Hossain and Floryan [4]. Fluid motion is driven by horizontal density gradients and occurs regardless of the intensity of the heating. Its pattern is determined by the externally imposed heating pattern unless transition to secondary states is encountered. The net heat transfer between the walls is driven by the nonlinear effects. The same heating applied to the moving fluid results in the reduction of drag experienced by this fluid. This so-called super-thermo-hydrophobic effect has been described in detail by Hossain et al. [5], where they demonstrate that spatially periodic heating helps to form small separation bubbles that isolate the moving stream from direct contact with the solid wall and thus reduce the shear stress acting on the fluid. The fluid movement inside separation bubbles is partially driven by the buoyancy gradients associated with the heating, which further contributes to the reduction of the required pressure drop.

Instead of simple sinusoidal heating, distributed bump like heating which occurs more frequently is focused in this study. This type of heating is introduced with a presumption that the heating would create separation bubbles in the flow system so that these bubbles help to enhance the heat transfer process. The lower wall is subjected to a spatially non-uniform heating distributed in the longitudinal direction so that it represents a sinusoidal-bump-like heating. The forcing generated by the heating is characterized by a wave number and amplitude, resulting in a two-parameter problem.

2. Problem formulation

A two-dimensional channel with height 2h as shown in Fig. 1 is considered in this study. The lower wall of the channel is subject to a spatial periodic sine-bump heating with temperatures of the lower (T_L) and upper (T_U) walls are specified as,

$$\begin{aligned} T_L(x) &= 0.5\cos(\alpha x) && 0 \le x \le \lambda/4 \\ &= 0 && \lambda/4 \le x \le 3\lambda/4 \qquad T_U(x) = 0 \\ &= 0.5\cos(\alpha x) && 3\lambda/4 \le x \le \lambda \end{aligned} \tag{1}$$

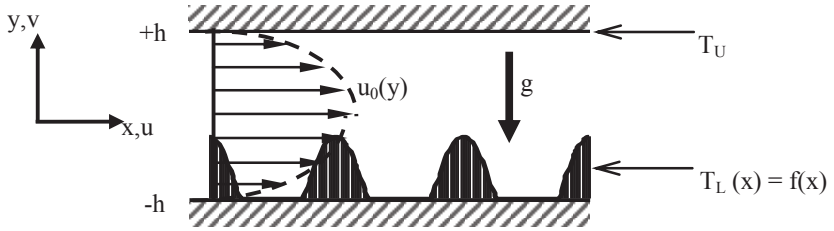

Figure 1.Sketch of the system configuration. Here, f(x) is a sinusoidal bump function as (1).

The velocity and pressure fields in the absence of any heating have the form of Poiseuille flow, and have the following form,

$$V(x,y) = [U_0(y),0] = [1-y^2,0], \qquad p_0(x,y) = -2x/\mathrm{Re} \tag{2}$$

Where **V**=(u,v) denotes the velocity vector scaled with the maximum of the x-velocity U_{max}, p_0 stands for the

pressure scaled with ρU_{max}^2, half-channel height h has been used as the length scale and the Reynolds number is defined as $Re=U_{max}h/\nu$.

The applied heating produces flow modifications that can be represented in the form

$$u_2(x,y) = \mathrm{Re}\,u_0(y) + u_1(x,y), \qquad v_2(x,y) = v_1(x,y),$$
$$T_2(x,y) = \mathrm{Pr}^{-1}\,T_0(x,y) + T_1(x,y), \qquad p_2(x,y) = \mathrm{Re}^2\,p_0(x,y) + p_1(x,y) \tag{3}$$

where (u_1,v_1), p_1 and T_1 stand for the velocity, the pressure and the temperature modifications due to the applied heating.

The dimensionless non-uniform conductive temperature field T_0 in (3) can be determined from the following problem

$$\partial^2 \mathrm{T}_0 / \partial \mathrm{x}^2 + \partial^2 \mathrm{T}_0 / \partial \mathrm{y}^2 = 0 \qquad \text{with boundary conditions (1).} \tag{4}$$

Solution of (4) has the form,

$$T_0(x,y) = \sum_{n=-\infty}^{+\infty} T_0^{(n)}(y) e^{in\alpha x}$$
$$= \sum_{n=-\infty}^{+\infty} \left[\frac{(T_U^{(n)} - T_L^{(n)})\sinh(n\alpha y)}{2\sinh(n\alpha)} + \frac{(T_U^{(n)} + T_L^{(n)})\cosh(n\alpha y)}{2\cosh(n\alpha)} \right] e^{in\alpha x} \tag{5}$$

With $T_L^{(0)} = 2/\pi, T_L^{(\pm n)} = 1/\pi(n^2-1)$ for $n \geq 0$ and $T_U^{(n)} = 0$ for $n \geq 1$

The dimensionless field equations describing motion of the incompressible-Newtonian fluid and changes in the temperature field have the form,

$$(\mathrm{Re}u_0 + u_1)\frac{\partial u_1}{\partial x_1} + \mathrm{Re}\,v_1 \frac{du_0}{dy} + v_1 \frac{du_1}{dy} = -\frac{\partial p_1}{dy} + \nabla^2 u_1 \tag{6a}$$

$$(\mathrm{Re}u_0 + u_1)\frac{\partial v_1}{\partial x} + v_1 \frac{dv_1}{dy} = -\frac{\partial p_1}{dy} + \nabla^2 u_1 + R\alpha T_1 + R\alpha\,\mathrm{Pr}^{-1}\,T_0 \tag{6b}$$

$$\mathrm{Pr}((\mathrm{Re}u_0 + u_1)\frac{\partial T_1}{\partial x} + v_1 \frac{dT_1}{dy}) + (\mathrm{Re}u_0 + u_1)\frac{\partial T_0}{\partial x} + v_1 \frac{dT_0}{dy} = \nabla^2 T_1 \tag{6c}$$

$$\frac{\partial u_1}{\partial x} + \frac{\partial v_1}{\partial y} = 0 \tag{6d}$$

where $Ra = g\Gamma h3Td/\nu k$ is the Rayleigh number, ∇^2 denotes the Laplace operator. The system is modeled with Boussinesq approximation which accounts the variation of density with temperature considering all other fluid properties to be constant [6].

The boundary conditions take the form

$$u_1(\pm 1) = 0, v_1(\pm 1) = 0, T_1(\pm 1) = 0, \tag{7}$$

The flow with or without the heating has to carry the same mass flow rate, i.e., fixed mass flow rate constraint. This constraint can be expressed as

$$Q=\int_{-1}^{1}u_2dy=\int_{-1}^{1}(\mathrm{Re}u_0+u_1)dy=\frac{4\mathrm{Re}}{3} \tag{8}$$

The complete problem, which consists of the field equations (6), the boundary conditions (7) and constraint (8), needs to be solved numerically.

3.Numerical Solution

To solve numerically we define the stream function ψ (x,y) in the usual manner, i.e., $u_1=\frac{\partial\psi}{\partial y}$

$v_1=-\frac{\partial\psi}{\partial x}$, and eliminate pressure from the momentum equations bringing the governing equations to the following form

$$\mathrm{Re}u_0\frac{\partial}{\partial x}(\nabla^2\psi)-\mathrm{Re}\frac{d^2u_0}{dy^2}\frac{\partial\psi}{\partial x}+N_\psi=\nabla^4\psi-Ra\frac{\partial T_1}{\partial x}-Ra\,\mathrm{Pr}^{-1}\frac{\partial T_0}{\partial x} \tag{9a}$$

$$\mathrm{PrRe}u_0\frac{\partial T_1}{\partial x}+\mathrm{Pr}N_{T_1}+\mathrm{Re}u_0\frac{\partial T_0}{\partial x}+N_{T_0}=\nabla^2T_1 \tag{9b}$$

where the nonlinear terms are written in the conservative form, i.e.

$$N_\psi=\frac{\partial}{\partial y}(\frac{\partial}{\partial x}\langle u_0,u_1\rangle)+(\frac{\partial}{\partial y}\langle u_1,v_1\rangle)-\frac{\partial}{\partial x}(\frac{\partial}{\partial x}\langle u_1,v_1\rangle+(\frac{\partial}{\partial y}\langle v_1,v_1\rangle),$$

$$N_{T_1}=\frac{\partial}{\partial x}\langle u_1,T_1\rangle+\frac{\partial}{\partial y}\langle v_1,T_1\rangle,\quad N_{T_0}=\frac{\partial}{\partial x}\langle u_1,T_0\rangle+\frac{\partial}{\partial y}\langle u_1,T_1\rangle$$

The solution is assumed to be in the form of Fourier expansions, i.e.

$$\psi(x,y)=\sum_{n=-\infty}^{+\infty}\psi^{(n)}(y)e^{in\alpha x},T_1(x,y)=\sum_{n=-\infty}^{+\infty}\psi^{(n)}(y)e^{in\alpha x}, \tag{10a}$$

$$u_1(x,y)=\sum_{n=-\infty}^{+\infty}u_1{}^{(n)}(y)e^{in\alpha x},v_1(x,y)=\sum_{n=-\infty}^{+\infty}v_1{}^{(n)}(y)e^{in\alpha x}, \tag{10b}$$

$$p_1(x,y)=A_px+\sum_{n=-\infty}^{+\infty}p_1{}^{(n)}(y)e^{in\alpha x} \tag{10c}$$

Where, $u_1{}^{(n)}=D\varphi^{(n)}$ and $v_1{}^{(n)}=in\alpha\varphi^{(n)}$ and A_p denotes pressure gradient modification.

Substitution of (10) into (9) and separation of Fourier components result in the following system of ordinary differential equations for the modal functions

$$D_n^2\varphi^{(n)}-in\alpha\,\mathrm{Re}(u_0D_n-\frac{d^2u_0}{dy^2})\varphi^{(n)}-in\alpha Ra\varphi^{(n)}=in\alpha Ra\,\mathrm{Pr}^{-1}T_0^{(n)}+N_\psi^{(n)} \tag{11a}$$

$$D_n\varphi^{(n)}-in\alpha\,\mathrm{PrRe}u_0\varphi^{(n)}=in\alpha\,\mathrm{Re}u_0T_0^{(n)}+N_{T_0}^{(n)}+\mathrm{Pr}N_{T_1}^{(n)} \tag{11b}$$

where $-\infty < n < +\infty, D = \frac{d}{dy}, D^2 = \frac{d^2}{dy^2}, D_n = D^2 - n^2\alpha^2$

$$N_{\psi}^{(n)} = in\alpha D\langle u_1, u_1\rangle^{(n)} + D^2\langle u_1, v_1\rangle^{(n)} + in^2\alpha^2\langle u_1, u_1\rangle^{(n)} - in\alpha D\langle v_1, v_1\rangle^{(n)}$$

$$N_{T_1}^{(n)} = in\alpha\langle u_1, T_1\rangle^{(n)} + D\langle v_1, T_1\rangle^{(n)},\ N_{T0}^{(n)} = in\alpha\langle u_1, T_0\rangle^{(n)} + D\langle v_1, T_0\rangle^{(n)}.$$

The linear terms have been placed on the left hand side, and the nonlinear and the known terms have been placed on the right hand side. The required boundary conditions for the modal functions have the form

$$D\varphi^{(n)}(\pm 1) = 0, \varphi^{(n)}(\pm 1) = 0, \text{ for } -\infty < n < +\infty \quad (12a,b)$$

$$\varphi^{(n)}(\pm 1) = 0, \text{ for } n \neq 0 \quad (12c)$$

$$\varphi^{(0)}(1) = M_1, \varphi^{(0)}(-1) = M_2, \quad (12d,e)$$

Where the constants M_1, M_2 can be selected arbitrarily [7]

In the case of the fixed mass flow rate constraint these constants have been selected in the form

$$\varphi^{(0)}(1) = 0, \varphi^{(0)}(-1) = 0, \quad (13a,b)$$

The system (11) together with the boundary conditions (12a-c) and either constraint (13a,b) needs to be solved numerically. For the purpose of numerical solution, expansions (10) have been truncated after N_M Fourier modes. The discretization method uses Chebyshev collocation technique based on N_T collocation points [8]. Gauss-Chebyshev-Lobatto points (Trefethen 2000) are used as the collocation points and their locations are computed from the following expression

$$y_k = \sin\left(\frac{\pi(N_T + 1 - 2k)}{2(N_T - 1)}\right), k = 0,1,2,\ldots,N_T \quad (14)$$

The resulting nonlinear algebraic system of equation is solved using an iterative technique combined with under-relaxation in the form

$$\Phi_{j+1} = \Phi_j + RF(\Phi_{comp} - \Phi_j) \quad (15)$$

Where $\Phi=\{\varphi^{(n)},\varphi^{(n)}\}$, Φ_{comp} denotes the current solution, Φ_j denotes the previous solution, and Φ_{j+1} stands for the accepted value of the next iteration and RF denotes the relaxation factor. Once solution of this problem has been completed, the first approximation of the nonlinear terms is computed on the basis of the available approximation of the velocity and temperature fields and system (11) is resolved with the new approximation of the nonlinear terms used on the RHS. This process is continued, with the update of the nonlinear terms taking place after each iteration, until a convergence criterion in the form

$$\max(\left|\Phi_{comp} - \Phi_j\right|) < TOL \quad (16)$$

is satisfied. TOL in denotes tolerance at two consecutive iterations. TOL set at 10^{-8} is found to be sufficient in most of the computations.

4. Results and discussions

Due to the presence of the external flow the present problem becomes a three-parameter problem, and the parameters are (i) the heating wave number α which dictates the spatial distribution of the heating, (ii) the Rayleigh number Ra which defines the intensity of the heating, and (iii) the Reynolds number Re which describes the strength of the external flow.

The structure of the conductive temperature field shown in **Fig. 2** demonstrates presence of large plumes at heating

wave number α =1 occupying almost the whole channel height. With the increase of heating wave number the height of this plume gradually reduces, and temperature distribution at the upper part of the channel becomes uniform which can easily be observed in Fig.2B. The conduction field creates non-uniform distribution of the buoyancy force along the length of the channel.

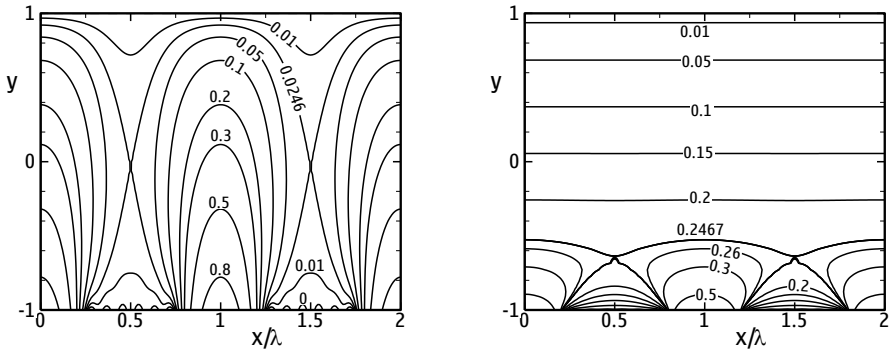

Figure 2.Isotherms of the conductive temperature field for the heating wave number α= 1(left) and α =10 (right).

With the presence of the above conduction field, when convection kicks in, the flow topology starts to evolve as shown in Fig. 3. For purely natural convection, (i.e. Re=0) the flow topology consists of counter rotating rolls (Fig. 3A). The fluid rises above the hot zones in the lower wall and descends above the non-heated zones forming pairs of counter-rotating rolls. When the external flow is introduced, flow topology starts to evolve away from the counter-rotating rolls, and streams of fluid starts to pass between the rolls. Figure 3B displays results for a weak external flow with Re = 1. The clock-wise rotating rolls are contained in the separation bubbles at the lower wall whereas the counter-clock-wise rolls are contained in the separation bubbles at the upper wall. This type of flow structure is usually observed at low Re, and when the intensity of heating is sufficiently high.

Further increase of flow strength washes away the upper-wall bubbles, retaining only the lower wall bubbles (Fig 3C). This type of flow structure occurs when the strength of flow Re is moderate, and intensity of heating Ra is sufficient to alter the bulk parallel motion of the fluids. In the lower wall some cold heavy fluids are trapped near the lower wall and isolated from the main stream flow and start to rotate.

When flow strength is sufficiently high and intensity of heating is sufficiently small, the lower-wall bubbles also disappear, and the flow becomes simple parallel flow (Fig. 3D). In this case, the intensity of heating cannot modify the bulk parallel motion of the fluid too much therefore we obtain very weak waviness in the flow stream. If the shear is further increased then the flow streamline becomes perfectly parallel.

The main quantity of interest is the heat transfer between the walls resulting from the convection. This heat transfer can be expressed in terms on the average Nusselt number Nu and defined as

$$\mathrm{Nu} = \frac{\mathrm{Pr}}{\lambda}\int_0^{\lambda}\left(-\left.\frac{\mathrm{d}\theta_1}{\mathrm{dy}}\right|_{y=-1}\right)\mathrm{dx} = -\mathrm{Pr}\left.\frac{\mathrm{d}\phi^{(0)}}{\mathrm{dy}}\right|_{y=-1} \tag{17}$$

Figure 4 shows the effect of heating intensity Ra on the heat transfer. It is evident that heat flow increases as the Rayleigh number Ra increases. Heat transfer is less for higher value of heating wave number (e.g., α=10). At higher α, convection prevails only near to the lower-heated wall, and at the upper part of the channel temperature changes linearly (see Fig. 2B) causing the heat to transport by conduction.

Figure 5 demonstrates the effect of strength of external flow Re on the heat transfer. Small Re flow is more efficient in heat transfer as Nu is higher in this region. Presence of upper and lower wall separation bubbles causes the hotter fluid to come in contact with the colder fluid easily thereby causes more heat to transport. With the increase of Re the size of the separation bubbles gradually reduces and eventfully disappear for high enough Re. The external flow

dominates the bulk parallel motion of the fluid, and the transverse heat transfer is limited to conduction only.

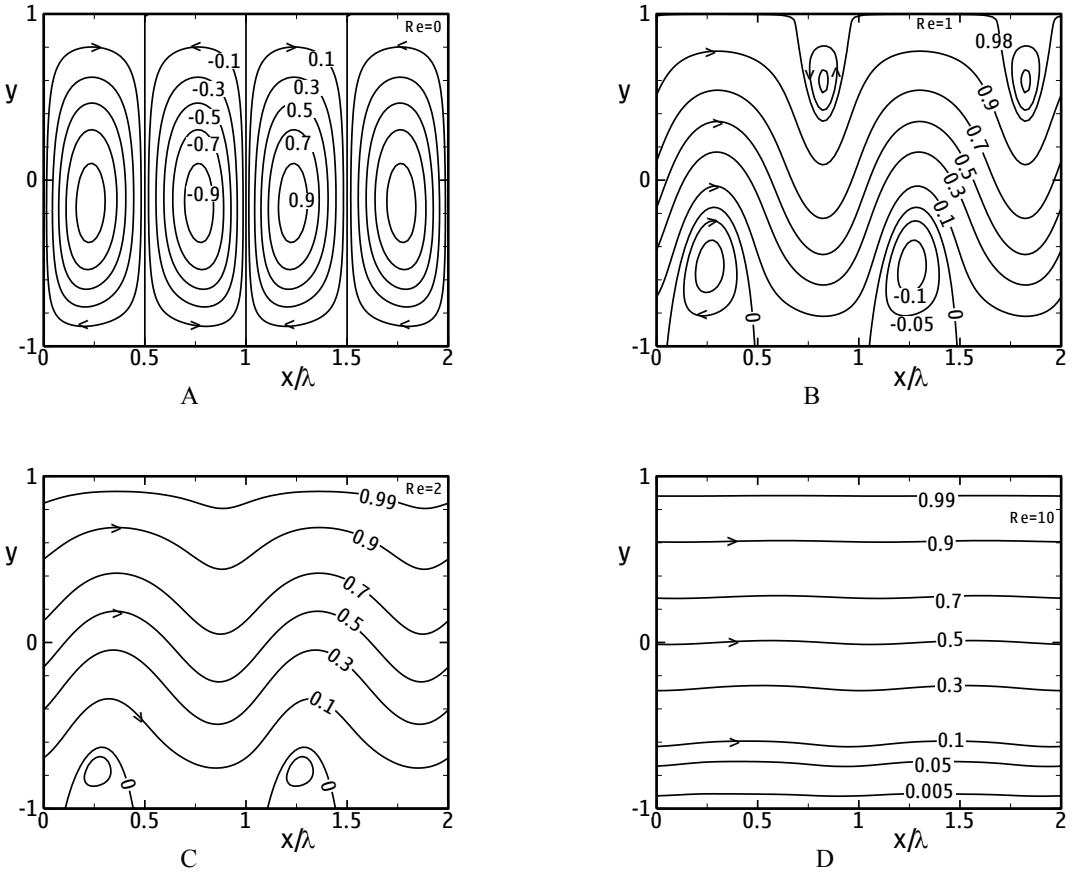

Figure 3. Flow topology for the Rayleigh number Ra = 100 and the heating wave number α = 2. Figures 3A-D correspond to the Reynolds number Re = 0, 1, 2, 10, respectively.

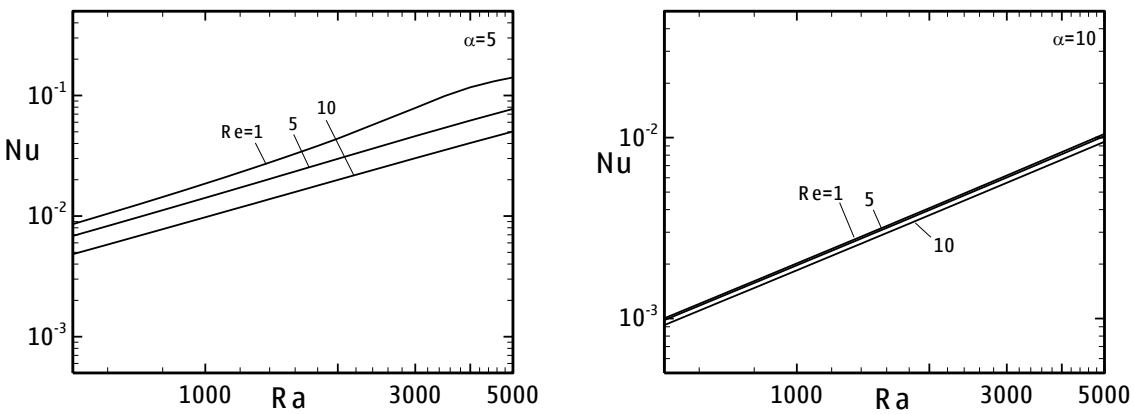

Figure 4. Variation of heat flow as a function of Rayleigh number Ra at selected values of the Reynolds number Re for the heating wave number α = 5 (left) and α = 10 (right).

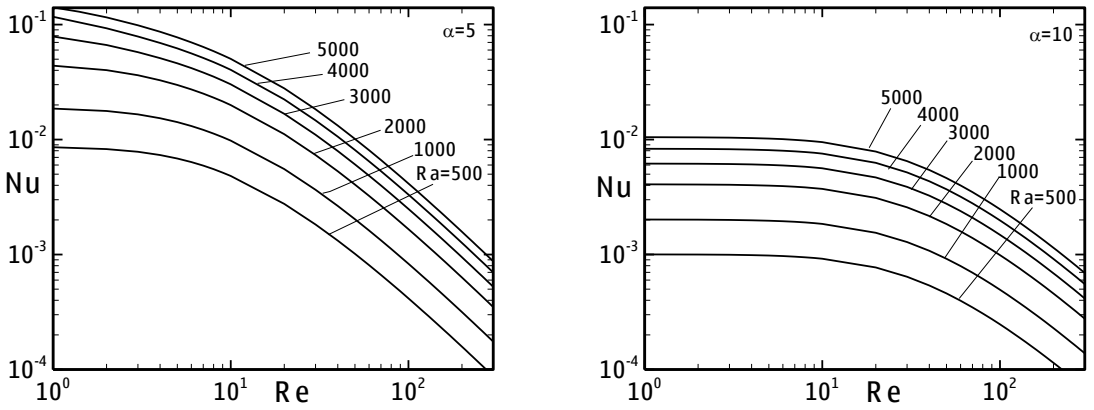

Figure 5: Variation of heat flow as a function of Reynolds number Re at selected values of the Rayleigh number Ra for the heating wave number $\alpha = 5$ (left) and $\alpha = 10$ (right).

To identify the heating pattern (i.e., the heating wave number α) which leads to the Maximum heat transfer, we refer to the plot shown in Fig.6. This figure shows that lower values of the heating wave number α provides more heat transfer than the higher values of α. When α is sufficiently high, Nu decreases proportional to α^{-3}, similar co-relation also reported by [3].

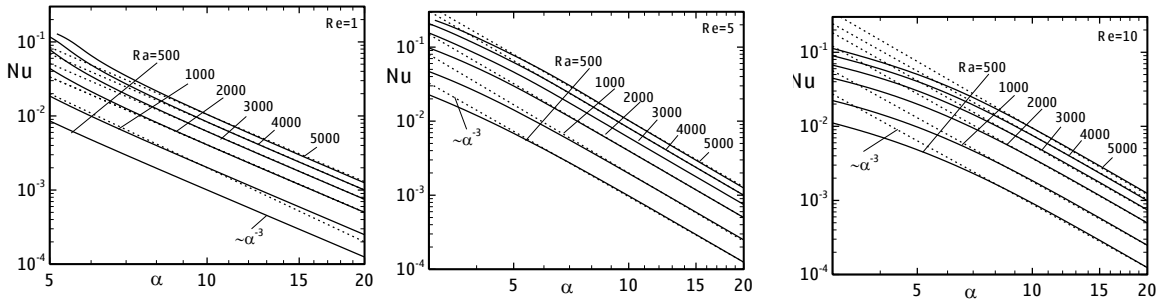

Figure 6: Variation of heat flow as a function of the heating wave number α at selected values of the Rayleigh number Ra for Reynolds number Re=1(left), 5(middle), and 10 (right).

5. Conclusion

Heat transfer characteristics due to the presence of spatially periodic sine-bump heating applied at the lower wall has been investigated. The convective flow structures provide separation bubbles either at upper wall, at lower wall or at both walls, depending on the heating wave number, intensity of heating, and strength of external flow. These separation bubbles are more active at low Reynolds number and at low heating wave number, thereby causing more heat transfer in this zone.

6. References

[1] Bodenschatz, E., Pesh, W. and Ahlers, G., "Recent developments in Rayleigh-Benard convection", Ann. Rev. Fluid Mech., 32, 709-778, 2000.
[2] Kelly, R. E., "The Onset and Development of Thermal Convection in Fully Developed Shear Flows", Advances In Applied Mechanics, vol31, pp. 35-112, 1994.

[3] Hossain, M. Z., "Convection due to spatially distributed heating", PhD Dissertation, The University of Western Ontario, London, ON, 2011.
[4] Hossain, M. Z., &Floryan, J. M., "Instabilities of Natural Convection in a Periodically Heated Layer". J. Fluid Mech., vol 733, pp. 33–67, 2013.
[5] Hossain, M. Z., Floryan, D. &Floryan, J. M., "Drag Reduction due to Spatial Thermal Modulations", J. Fluid Mech., vol 713, pp. 398–419, 2012.
[6] Chandrasekhar, S., Hydrodynamic and Hydromagnetic Stability. Oxford University Press, 1961.
[7] Floryan, J.M., 1997, Stability of wall bounded shear layers with simulated distributed surface roughness, J. Fluid Mech., 335, 29-55.
[8] Canuto, C., Hussaini, M.Y., Quarteroni, A., Zang, T.A., Spectral Methods, Springer, 1996.